Theoretical Estimation of the Solvent Effect of the Lithium Isotopic Reduced Partition Function Ratio

Hidekazu Watanabe,* Kazuyo Yamaji, Akinari Sonoda, Yoji Makita, Hirofumi Kanoh, and Kenta Ooi*

National Institute of Advanced Industrial Science and Technology, Hayashi-cho 2217-14, Takamatsu, Kagawa, 761-0395, Japan

Received: January 31, 2003; In Final Form: July 15, 2003

The reduced partition function ratios (RPFRs) of $Li^+(Solv)_n$ (in which Solv = H_2O, H_2S, and CH_3OH) clusters with different values were calculated, to investigate the solvent effect of the isotopic effect of the lithium. Structures of three solvated clusters—$Li^+(H_2O)_n$, $Li^+(H_2S)_n$, and $Li^+(CH_3OH)_n$—were optimized by an ab initio molecular orbital method, and their RPFRs were calculated by frequency analysis. The RPFR of the solution was estimated by the extrapolation of the cluster values. The most-stable isomers of all three clusters for $n \geq 4$ have four solvent molecules in their first shell. The RPFR is dependent mainly on the number of solvent molecules in the first shell, and the size dependence of the RPFR plateaus at $n = 4$. The extrapolation of these values can be regarded as the RPFR in the solutions. The RPFRs are ~1.07 for $Li^+(H_2O)_n$ and $Li^+(CH_3OH)_n$ and are ~1.03 for $Li^+(H_2S)_n$. The smaller RPFR of $Li^+(H_2S)_n$ is attributed to the smaller binding energy of the Li−S bond, which is weaker than that of the Li−O bond. The present results suggest the possibility of ionophores with S atoms (such as thioether, etc.) for lithium isotopic separation.

1. Introduction

The Li atom has two types of stable isotopes whose masses are six and seven. The light but minor isotope ^6Li is expected to be capable of nuclear reaction, and it is important to establish the technology for the separation of the minor isotope ^6Li from an isotope mixture that contains the major isotope ^7Li. It is also important to study lithium isotopic fractionation as a fundamental material and from the viewpoint of geological science. Lithium isotopic fractionation through chemical exchanges between the two phases has been studied in various systems, such as lithium amalgam, lithium metal, organic and inorganic ion exchangers, macrocyclic polyether, and membranes.[1−8] The highest fractionation ability was obtained in the lithium isotopic exchange reaction between an aqueous solution phase and an amalgam phase, where the separation factor was 1.05.[5]

The reaction of the lithium isotopic exchange between the two phases is written as

$$^6Li_I^+ + {}^7Li_{II}^+ \rightleftharpoons {}^7Li_I^+ + {}^6Li_{II}^+ \quad (1)$$

The separation factor (S) is the equilibrium constant of this isotopic exchange reaction (eq 1), and S can be given by the reduced partition function ratio $S = f_I/f_{II}$, where f_I and f_{II} are the reduced partition function ratios (RPFRs) of the lithium species in phases I and II. The RPFR (f) for each phase is given by Bigeleisen and Mayer's theory,[9] as follows:

$$f = \prod_i \frac{u_{i,(H)} e^{-u_{i,(H)}/2}(1 - e^{-u_{i,(L)}})}{u_{i,(L)} e^{-u_{i,(L)}/2}(1 - e^{-u_{i,(H)}})} \quad (2)$$

and the indices (H) and (L) correspond to the heavy and light isotopes, respectively. The index i in eq 2 corresponds to the value of the ith normal mode. The value of u_i in the equation consists of Plank's constant h, Boltzmann's constant k_B, absolute temperature T, and the normal frequency of the ith mode ω_i:

$$u_i = \left(\frac{h}{k_B T}\right)\omega_i$$

Bigeleisen and Mayer also derived a simple theory for the estimation of the RPFR, using an experiment that involved a Raman active spectrum. Estimation of a reasonable RPFR for the Li ion in dilute solution with an experimental method has been difficult, although Raman spectroscopy for hydrated Li ions has been extensively studied.[10−13]

Recent progress in theoretical chemistry makes it possible to evaluate the RPFR (f) by the calculation of the frequencies ω_i with computational methods such as Monte Carlo (MC), molecular dynamics (MD), and ab initio molecular orbital (MO) methods.[14−19] The RPFR can be predicted theoretically by a Bigeleisen and Mayer formula if we can calculate all the frequencies ω_i of the given system, and it is well-known that all harmonic frequencies can be conventionally calculated by an ab initio MO method.

The hydrated clusters of the lithium cation and other alkali-metal cations have been well investigated by an ab initio MO method,[20−30] and their structures and other properties are well-known. Previously, we investigated the structure of the hydrated lithium ion cluster $Li^+(H_2O)_n$ (up to $n = 6$) by an ab initio MO method and estimated the RPFR of the isotope exchange reaction of the Li atom in a water solution.[19] The RPFR (f) in the water solution is estimated by the extrapolation of the RPFR of the cluster, up to $n = 6$.

Several types of solvated alkali-metal cation clusters other than hydrated clusters have also been investigated with an ab initio MO method.[13,17,18,20,21,24−26,28−30] The RPFR and the

* Authors to whom correspondence should be addressed. E-mail: watanabe.h@aist.go.jp, k-ooi@aist.go.jp.

10.1021/jp0301507 CCC: $25.00
Published on Web 08/29/2003

TABLE 1: Scaling Factor Uniformly Applied to the Calculated Frequencies

	basis set (*)[a]	HF/6-31+G*	HF/6-31+G**	HF/6-311+G*
H_2O		0.8941	0.8943	0.8835
H_2S		0.9190	0.9208	0.9379
MeOH	0.9225	0.9191		

[a] Basis set (*) is HF/6-31G on the CH_3 group of the methanol molecule and HF/6-31+G* on the other atoms.

reduced statistical sums (β-factor) have been calculated for some of the solvated Li cation clusters.[17,18,28] Nielsen et al. investigated the competitive reaction of alkali-metal ions with water and methanol $M^+(H_2O)_n(CH_3OH)_m$ in the gaseous phase,[30] whereas, in a study using MD simulation, Lisy's group investigated the alkali-metal cations with methanol clusters $Cs^+(CH_3OH)_n$ and $Na^+(CH_3OH)_n$.[31−34]

However, there are no reports on the Li cation with only methanol molecules $Li^+(CH_3OH)_n$, using an ab initio MO calculation. In the present study, we calculated the RPFRs of the $Li^+(CH_3OH)_n$ clusters and estimated the RPFR in the methanol solution via extrapolation of the cluster value. We also studied the RPFR of the $Li^+(H_2S)_n$ clusters, for which there has been no investigation with an ab initio MO calculation. In particular, we hypothesize that the result with $Li^+(H_2S)_n$ suggests the possibility of an absorbent that involves S atoms such as thioether.

Comparing the RPFRs of $Li^+(CH_3OH)_n$ and $Li^+(H_2S)_n$ with the hydrated lithium cation $Li^+(H_2O)_n$, we have discussed the solvent effect of the RPFR. The structure of $Li^+(H_2O)_n$ clusters has been well investigated in previous studies.[13,18,19,23−30] We found more isomers of $Li^+(H_2O)_n$ in this study than in the previous study.[19] We also studied the thermochemistry for their isomerization and have included a detailed discussion about the stability and the influence of the estimated RPFR in bulk solutions.

2. Computational Methods

The geometric structures of three types of solvated Li ion clusters—$Li^+(H_2O)_n$, $Li^+(H_2S)_n$, and $Li^+(CH_3OH)_n$—were optimized by an ab initio MO method, up to $n = 6$. The optimization was performed with three types of basis sets—the HF/6-31+G*, HF/6-31+G**, and HF/6-311+G* levels—for $Li^+(H_2O)_n$ and $Li^+(H_2S)_n$. Two types of basis set were used for the optimization of $Li^+(CH_3OH)_n$: in basis set (1), the 6-31+G* basis set was applied to all the atoms, whereas in basis set (2), the 6-31G basis set was applied to the methyl groups and the 6-31+G* set was applied to the other groups/atoms. Basis set (2) is denoted hereafter as "basis set (*)".

The normal frequencies were evaluated at every optimized structure, and we have ascertained that all structures found are the true local minimum. The calculated normal frequencies were multiplied uniformly with a scaling factor to enable qualitative discussion. Because there is no experimental data for the frequency that involves the vibration mode of the Li^+−Solv bond, the scaling factor was determined from the experimental data for isolated water, hydrogen sulfide (H_2S), and methanol.[35] Table 1 summarizes the scaling factors, and the RPFRs are evaluated with these scaled frequencies. The typical scaling factors of the Hartree−Fock (HF) level, ~0.9, were obtained. The thermodynamic properties were evaluated under the assumption of the ideal gas. The program used for the ab initio MO calculations was the GAUSSIAN 98 program.[36]

3. Results and Discussion

3.1 Structures. *3.1.1 Structure of $Li^+(H_2O)_n$.* Figure 1 shows the fully optimized geometries of the $Li^+(H_2O)_n$ clusters, up to $n = 4$. The fully optimized structures of several isomers of $Li^+(H_2O)_5$ and $Li^+(H_2O)_6$ are shown in Figures 2 and 3, respectively. Bond lengths of the several dominant parts are drawn in the figures. The Cartesian coordinates of all optimized geometries are available on request.[37] Table 2 summarizes the

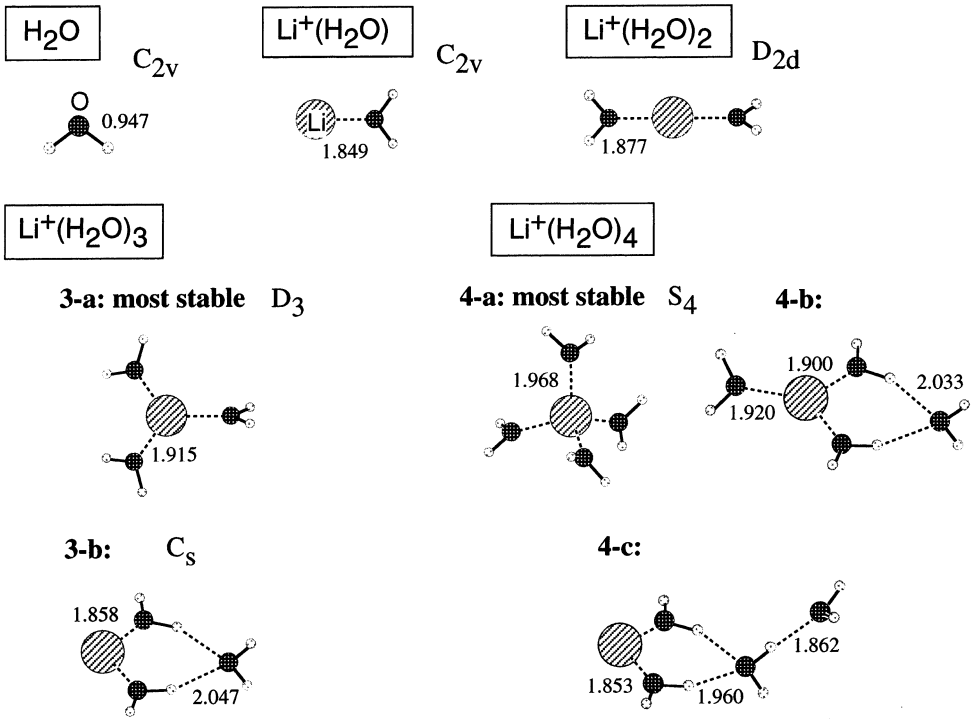

Figure 1. Optimized structures of clusters $Li^+(H_2O)_n$ ($1 \le n \le 4$). Bond lengths of the dominant part are shown in the HF/6-31+G* level, and the units are given in angstroms.

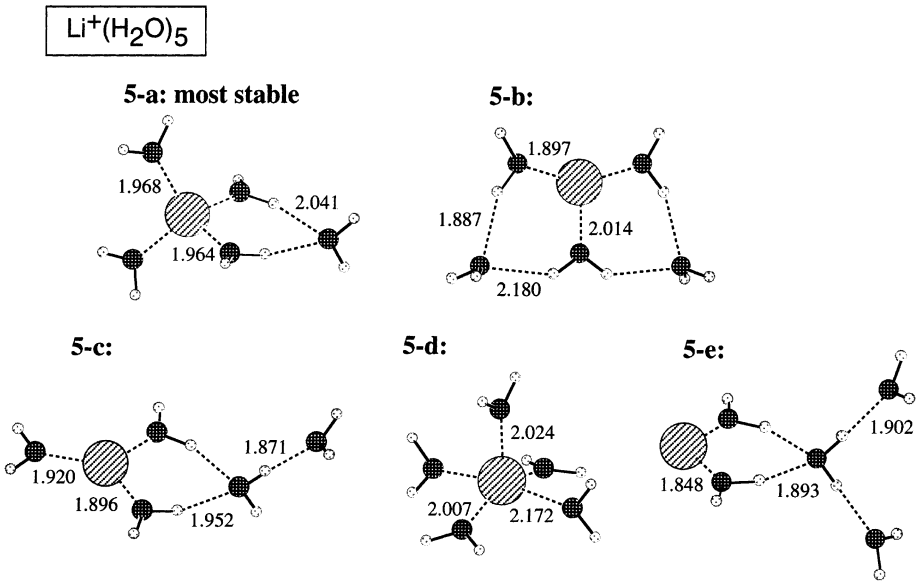

Figure 2. Optimized structures of clusters $Li^+(H_2O)_5$. Bond lengths of the dominant part are shown in the HF/6-31+G* level, and the units are given in angstroms.

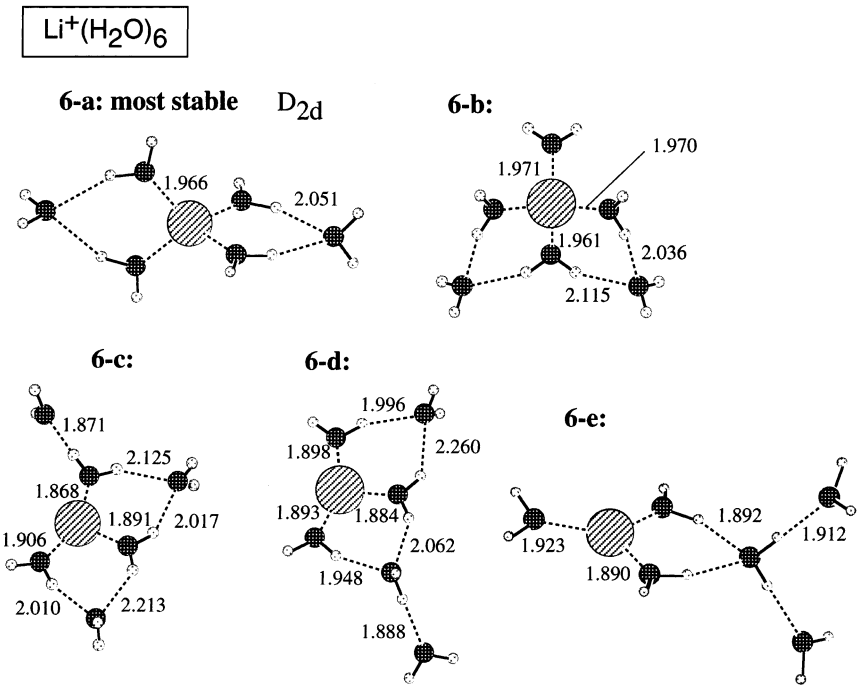

Figure 3. Optimized structures of clusters $Li^+(H_2O)_6$. Bond lengths of the dominant part are shown in the HF/6-31+G* level, and the units are given in angstroms.

relative energy difference with and without the zero-point vibration energy correction, ($\Delta E_{iso}^{(7)}$ and ΔE_{iso}), evaluated with three basis sets. The Gibbs' free energy change ($\Delta G_{iso}^{(7)}$) at room temperature (298.15 K) is also summarized in the table. We calculated the $\Delta E_{iso}^{(7)}$ and $\Delta G_{iso}^{(7)}$ values for the case of the dominant isotope ^{7}Li. The case of the minor isotope ^{6}Li is not shown here, because the energy difference is very small (less than ~1 kJ/mol)

In this paper, the structure $Li^+(Solv)_p(Solv)_q$ is hereafter denoted as $p+q$, where p and q are the numbers of solvent molecules in the first and external solvent shells, respectively.[23,25]

The most-stable isomer, up to $n = 4$, has the $n+0$ structure, and all water molecules are directly bound to the Li ion equivalently. This is characteristic of the system in which the central metal ion has no valence electron. The hydration of the $(MgOH)^+(H_2O)_n$ is similar, because there is no valence electron around the Mg atom, because of delocalization by polarization of a $MgOH^+$ molecular ion.[38,39] In contrast, the structure of the entire cluster becomes a pyramid type if there is one valence electron at the central metal, such as neutral $Li(H_2O)_n$, $Na(H_2O)_n$,[20−22] and singly charged $Mg^+(H_2O)_n$.[38−41]

For $n \geq 4$, the most-stable isomer has a $4+q$ structure, in which four water molecules exist in the first hydration shell. The water molecule of the second shell forms a cyclic structure that is constructed with hydrogen bonds to two water molecules in the first shell. The next-stable isomer has a $3+q$ isomer, whereas the $2+q$ isomer is much less stable. These isomers also have a cyclic structure with two hydrogen bonds, making the entire cluster stable. As mentioned in Section 3.2, the hydrogen

TABLE 2: Relative Energy Difference without the Zero-Point Vibration Energy Correction (ΔE_{iso}) and with the Correction ($\Delta E_{iso}^{(7)}$) and the Relative Gibbs' Free Energy Change ($\Delta G_{iso}^{(7)}$) of Isomers of $Li^+(H_2O)_n$[a]

		HF/6-31+G*			HF/6-31+G**			HF/6-311+G*		
	$p+q$	ΔE_{iso}	$\Delta E_{iso}^{(7)}$	$\Delta G_{iso}^{(7)}$	ΔE_{iso}	$\Delta E_{iso}^{(7)}$	$\Delta G_{iso}^{(7)}$	ΔE_{iso}	$\Delta E_{iso}^{(7)}$	$\Delta G_{iso}^{(7)}$
					$Li^+(H_2O)_3$					
3-a	3+0	0.00	0.00	0.00	0.00	0.00	0.00	0.00	0.00	0.00
3-b	2+1	38.74	44.26	46.60	39.79	44.81	46.37	41.53	46.58	47.93
					$Li^+(H_2O)_4$					
4-a	4+0	0.00	0.00	0.00	0.00	0.00	0.00	0.00	0.00	0.00
4-b	3+1	8.63	15.13	18.74	9.84	15.49	17.24	9.65	16.50	20.79
4-c	2+2	58.89	67.08	71.05	60.46	67.99	70.42	61.92	70.38	75.84
					$Li^+(H_2O)_5$					
5-a	4+1	0.00	0.00	0.00	0.00	0.00	0.00	0.00	0.00	0.00
5-b	3+2	11.76	16.15	19.02	12.24	16.34	18.50	12.52	17.57	21.17
5-c	3+2	17.85	19.40	11.52	18.34	19.92	13.36	17.84	20.76	16.41
5-d	5+0	22.95	17.04	13.40	23.31	17.36	13.27	22.58	18.70	18.46
5-e	2+3	73.13	75.11	69.16	73.69	75.79	70.33	75.90	78.82	75.25
					$Li^+(H_2O)_6$					
6-a	4+2	0.00	0.00	0.00	0.00	0.00	0.00	0.00	0.00	0.00
6-b	4+2	5.74	5.76	2.52	5.97	5.72	1.75	6.82	5.88	0.68
6-c	3+3	18.75	19.59	12.03	18.76	19.58	11.59	19.97	21.44	14.05
6-d	3+3	20.01	21.78	14.24	20.45	22.24	14.42	20.67	23.11	15.85
6-e	3+3	30.84	28.83	14.52	31.03	29.19	14.28	31.44	30.40	16.77

[a] The values are expressed in units of kJ/mol. The case of the dominant isotope ^{7}Li is calculated for $\Delta E_{iso}^{(7)}$ and $\Delta G_{iso}^{(7)}$. The Gibbs' function $\Delta G_{iso}^{(7)}$ is evaluated at 298.15 K, under the assumption of the ideal gas.

TABLE 3: Relative Energy Differences (ΔE_{iso} and $\Delta E_{iso}^{(7)}$) and the Relative Gibbs' Free Energy Change ($\Delta G_{iso}^{(7)}$) of Isomers of $Li^+(H_2S)_n$ for the Dominant Isotope ^{7}Li[a]

		HF/6-31+G*			HF/6-31+G**			HF/6-311+G*		
	$p+q$	ΔE_{iso}	$\Delta E_{iso}^{(7)}$	$\Delta G_{iso}^{(7)}$	ΔE_{iso}	$\Delta E_{iso}^{(7)}$	$\Delta G_{iso}^{(7)}$	ΔE_{iso}	$\Delta E_{iso}^{(7)}$	$\Delta G_{iso}^{(7)}$
					$Li^+(H_2S)_4$					
4-a	4+0	0.00	0.00	0.00	0.00	0.00	0.00	0.00	0.00	0.00
4-b	3+1	22.38	21.37	14.51	21.94	21.09	14.98	21.65	22.89	13.18
					$Li^+(H_2S)_6$					
6-a	4+2	0.00	0.00	0.00	0.00	0.00	0.00	0.00	0.00	0.00
6-b	4+2	1.75	1.63	−1.48	1.84	1.66	−1.50	2.15	1.82	0.50

[a] The values are given in units of kJ/mol. The Gibbs' function is evaluated at 298.15 K, under the assumption of the ideal gas.

bond between water molecules is weaker than the Li^+−water bonding, and the isomers of $3+q$ and $2+q$ are, therefore, not the most-stable structure.

The cyclic structure is rigid; therefore, the number of low-frequency modes becomes smaller, and, thus, the correction for the zero-point vibration energy is significant. In the reactions of **3-a** → **3-b** and **4-a** → **4-b**, the corrected relative energy difference $\Delta E_{iso}^{(7)}$ is ∼5−7 kJ/mol larger than ΔE_{iso}. The Gibbs' free energy change at room temperature, $\Delta G_{iso}^{(7)}$, is ∼6−8 kJ/mol higher than ΔE_{iso}. The cyclic structure makes the entropy effect small.

In the $Li^+(H_2O)_5$ clusters, the most-stable isomer is **5-a** with a 4+1 structure, whereas isomers **5-b** and **5-c** with a 3+2 structure are the next stable. Isomer **5-b** is more stable than isomer **5-c** in the relative energy $\Delta E_{iso}^{(7)}$; however, their stability reverses in the Gibbs' function $\Delta G_{iso}^{(7)}$, because of the rigid hydrogen bond network with the small entropy in isomer **5-b**. We also found a stable local minimum in the 5+0 structure (isomer **5-d**) at all three basis sets (HF/6-31+G*, HF/6-31+G**, and HF/6-311+G*). Although isomer **5-d** is much more stable than isomer **5-e** with a 2+3 structure, Pye noticed the fact that the isomer of **5-d** type does not have a stable local minimum, as calculated using the second-order Möller−Plesset perturbation theory (MP2) with the 6-31+G* basis set.[26] It suggests the large dependence of the calculation level on the existence of the local minimum for the $5+q$ structure.

We found two 4+2 structures for $Li^+(H_2O)_6$. Isomer **6-b** is distorted by the hydrogen bond network and is ∼5−6 kJ/mol less stable than isomer **6-a**. However, the relative Gibbs' free energy change becomes almost zero in the isomerizartion of **6-a** → **6-b**, because of the entropy change $\Delta S > 0$ that is caused by the distorted hydrogen bond network and one free water molecule in isomer **6-b**. For the 3+3 structure, three isomers (**6-c**, **6-d,** and **6-e**) were found, with isomer **6-e** being less stable than other two in $\Delta E_{iso}^{(7)}$. However, the Gibbs' free energy change $\Delta G_{iso}^{(7)}$ is almost zero among the three 3+3 isomers, because of the large entropy by the free water molecules in isomer **6-e**. Finally, the Gibbs' function of the isomerization reaction for $n = 6$ is dependent almost entirely on the coordination number of the first hydration shell.

3.1.2. Structure of $Li^+(H_2S)_n$. The optimized geometric structures of $Li^+(H_2S)_n$, up to $n = 6$, are shown in Figure 4. Table 3 summarizes the relative energy differences ΔE_{iso} and $\Delta E_{iso}^{(7)}$, as well as the Gibbs' free energy change $\Delta G_{iso}^{(7)}$ that has been evaluated with three basis sets—HF/6-31+G*, HF/6-31+G**, and HF/6-311+G*—at room temperature (298.15 K).

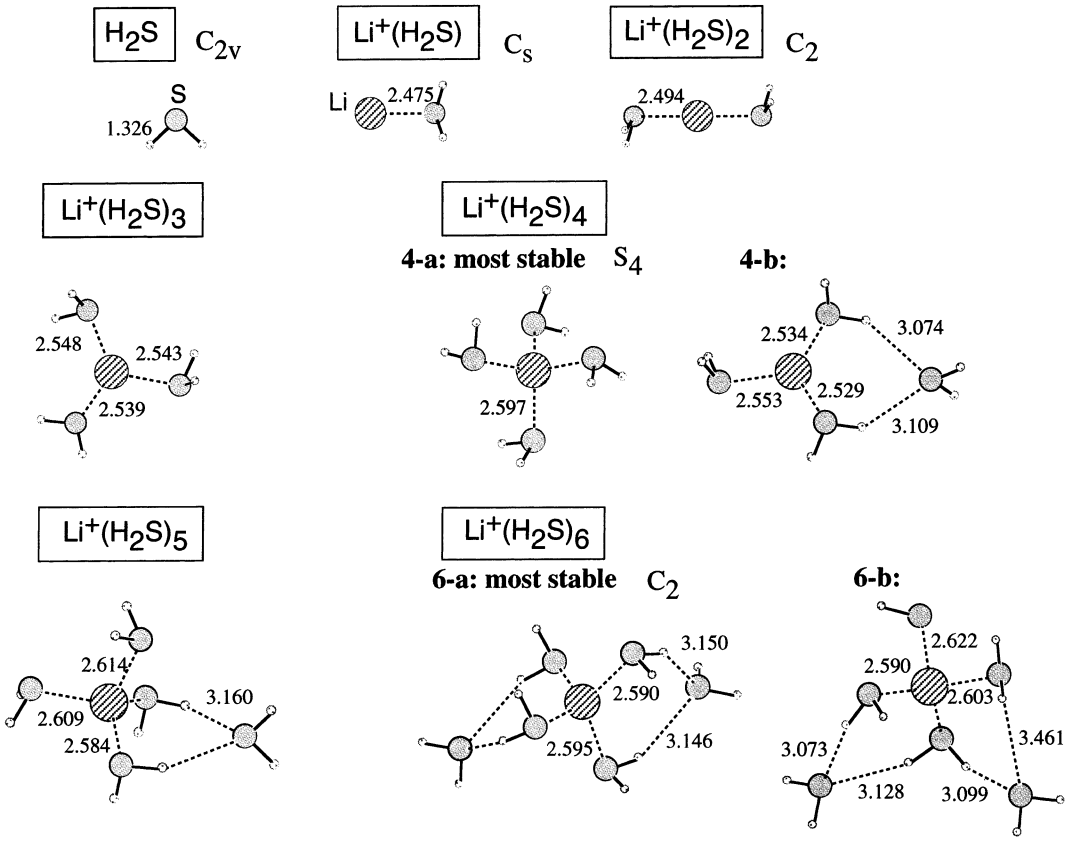

Figure 4. Optimized structures of clusters $Li^+(H_2S)_n$, up to $n = 6$. Bond lengths of the dominant part are shown in the HF/6-31+G* level, and the units are given in angstroms.

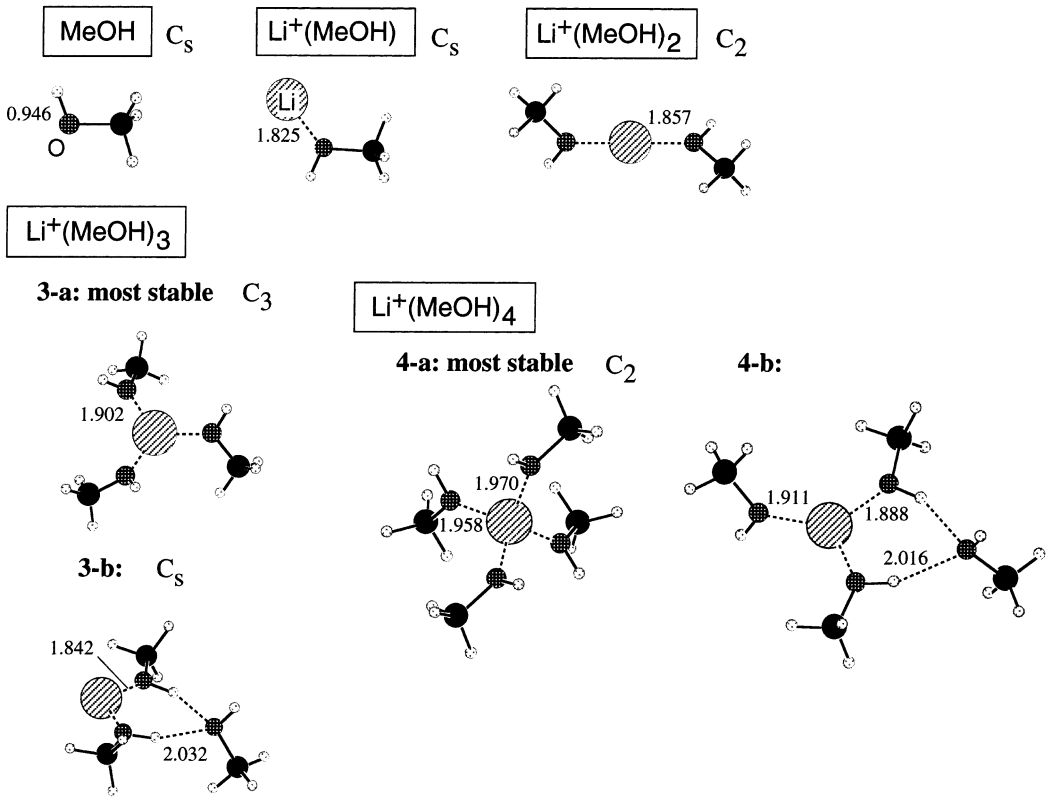

Figure 5. Optimized structures of clusters $Li^+(CH_3OH)_n$, up to $n = 4$. Bond lengths of the dominant part are shown in the HF/6-31+G* level, and the units are given in angstroms.

The stability of $Li^+(H_2S)_n$ is significantly different from that of $Li^+(H_2O)_n$. The length of the Li−S bonds is ∼2.5 Å and is longer than that of Li−O. The hydrogen bonds between H_2S molecules are longer than 3 Å and are also longer than the length of the hydrogen bond between water molecules. The interaction involving the S atom is very weak.

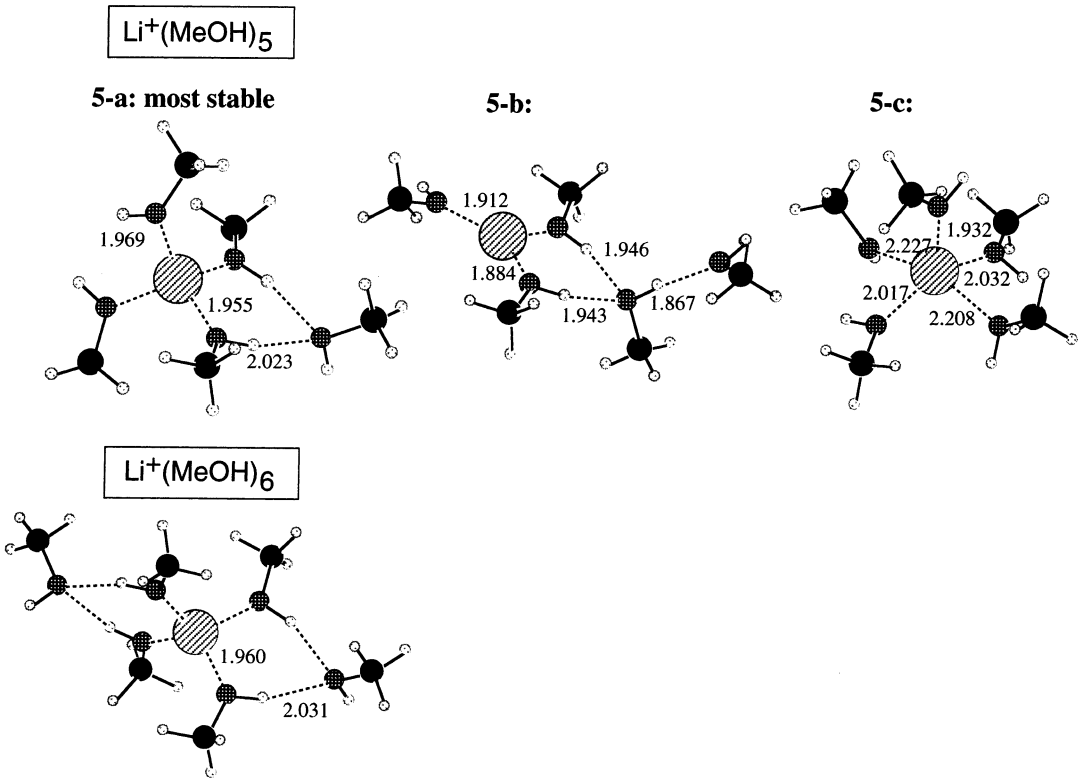

Figure 6. Optimized structures of clusters $Li^+(CH_3OH)_5$ and $Li^+(CH_3OH)_6$ Bond lengths of the dominant part are shown in the HF/6-31+G* level, and the units are given in angstroms.

The most-stable isomer, up to $n = 4$, has an n+0 structure, and a 4+q structure is observed for $n \geq 4$. The coordination number of $Li^+(H_2S)_n$ is the same as for $Li^+(H_2O)_n$, but there is less variation in the possible isomers in the $Li^+(H_2S)_n$ cluster, because of the instability due to the weak interactions. For $n =$ 3, only the 3+0 structure can exist, and we could not find a stable local minimum for the 2+1 structure, which has a second solvent shell. We could find only two isomers (4+0 and 3+1) for $n = 4$ and two 4+2 isomers for $n = 6$.

The entropy effect on the isomerization reaction of $Li^+(H_2S)_n$ is quite different from that of $Li^+(H_2O)_n$. In the isomerization of **4-a** → **4-b** for $Li^+(H_2S)_4$, the Gibbs' free energy change $\Delta G^{(7)}_{iso}$ is smaller than the relative energy differences $\Delta E^{(7)}_{iso}$. It is assumed that the H_2S molecule in the second shell of isomer **4-b** retains large entropy, because it is permitted a large degree of freedom, which is attributable to the weakness of the hydrogen bond to the first shell. The relative energy differences (ΔE_{iso} and $\Delta E^{(7)}_{iso}$) are almost zero between the two isomers of $Li^+(H_2S)_6$. In comparison with $Li^+(H_2O)_6$, the hydrogen bonds of $Li^+(H_2S)_6$ are weaker, whereas low-frequency modes are retained and the structural distortion is not so significant.

3.1.3. Structure of $Li^+(CH_3OH)_n$. Figures 5 and 6 show the optimized geometries of the $Li^+(CH_3OH)_n$ cluster. Table 4 summarizes the basis set dependences of the relative energy differences ΔE_{iso} and $\Delta E^{(7)}_{iso}$ and the Gibbs' function $\Delta G^{(7)}_{iso}$ at room temperature (298.15 K).

The stability and structure of $Li^+(CH_3OH)_n$ are similar to those of $Li^+(H_2O)_n$. The zero-point vibration energy correction and the influence of the entropy are smaller, because a methanol molecule cannot make two hydrogen bonds in the form of a double proton donor, and the difference between $\Delta E^{(7)}_{iso}$ and ΔE_{iso} or $\Delta G^{(7)}_{iso}$ and ΔE_{iso} is not as significant as that in the case of $Li^+(H_2O)_n$. For example, in $Li^+(CH_3OH)_5$, the Gibbs' function $\Delta G^{(7)}_{iso}$ of the 5+0 isomer (**5-c**) has much higher energy than that of the 3+2 isomer (**5-b**). This trend is different from the case of $Li^+(H_2O)_5$, in which the difference of $\Delta G^{(7)}_{iso}$ is almost zero in the 5+0 and 3+2 isomers.

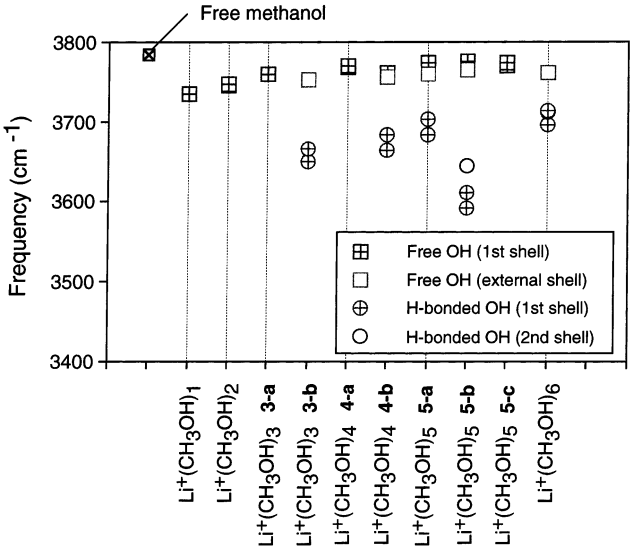

Figure 7. Calculated frequencies of $Li^+(CH_3OH)_n$ in the region of the OH stretching motion at the HF/6-31+G* level. A scaling factor of 0.9191 is applied.

Lisy's group investigated the infrared (IR) spectra of $Na^+(CH_3OH)_n$ and $Cs^+(CH_3OH)_n$ in the frequency region of the OH stretching motion.[32−34] Their results suggest that the most-stable isomer has an n+0 structure, which is the same as $Li^+(H_2O)_n$. Figure 7 shows the calculated frequencies of the OH stretching motion of the $Li^+(CH_3OH)_n$ clusters, and the frequency identified as free OH is in the region of ∼3750 cm^{-1}. Lisy's group observed one peak of free OH stretching motion in the region of ∼3660−3670 cm^{-1} for $n \geq 4$ of $Na^+(CH_3OH)_n$ and $Cs^+(CH_3OH)_n$.

TABLE 4: Relative Energy Differences (ΔE_{iso} and $\Delta E_{iso}^{(7)}$) and the Relative Gibbs' Free Energy Change ($\Delta G_{iso}^{(7)}$) of Isomers of $Li^+(CH_3OH)_n$ for the Dominant Isotope ^7Li[a]

		Basis Set (*)[b]			HF/6-31+G*		
	$p+q$	ΔE_{iso}	$\Delta E_{iso}^{(7)}$	$\Delta G_{iso}^{(7)}$	ΔE_{iso}	$\Delta E_{iso}^{(7)}$	$\Delta G_{iso}^{(7)}$
				$Li^+(MeOH)_3$			
3-a	3+0	0.00	0.00	0.00	0.00	0.00	0.00
3-b	2+1	42.26	45.61	48.21	40.84	44.22	47.49
				$Li^+(MeOH)_4$			
4-a	4+0	0.00	0.00	0.00	0.00	0.00	0.00
4-b	3+1	5.25	10.02	11.96	6.22	10.49	10.12
				$Li^+(MeOH)_5$			
5-a	4+1	0.00	0.00	0.00	0.00	0.00	0.00
5-b	3+2	16.54	18.21	11.08	16.39	17.90	10.62
5-c	5+0	30.55	26.31	23.67	29.18	24.99	23.25

[a] The values are given in units of kJ/mol. The Gibbs' function is evaluated at 298.15 K, under the assumption of the ideal gas. [b] The basis set (*) is the 6-31G set on the CH_3 groups of the methanol and the 6-31+G* sets on the other atoms.

They also suggest the existence of a surface-type structure for $n \geq 3$, in which the Na^+ or Cs^+ are on the cyclic $(CH_3OH)_n$ cluster. We could not find such a surface structure in $Li^+(CH_3OH)_n$. Considering the stability in the alkali-metal cation with a water cluster,[24,25] the Li−methanol bond is much stronger than the Na−methanol and Cs−methanol bonds; thus, the $Li^+(CH_3OH)_n$ cluster cannot have a stable local minimum.

3.2. Solvation Energy and Gibbs' Function. Figure 8 shows the size dependence of the solvation energy $\Delta E_{solv}^{(7)}$, which involves the zero-point vibration energy correction and the Gibbs' free energy change $\Delta G_{solv}^{(7)}$ at room temperature (298.15 K) for the most-stable isomers. The solvation reaction is

$$Li^+(Solv)_{n-1} + Solv \rightarrow Li^+(Solv)_n \quad (\text{for Solv} = H_2O, H_2S, \text{and } CH_3OH) \quad (3)$$

The horizontal broken lines show the dimerization energy and the Gibbs' function of $(H_2O)_2$, $(CH_3OH)_2$, and $(H_2S)_2$. The calculation level is HF/6-31+G*. The energy differences $\Delta E_{solv}^{(7)}$ and $\Delta G_{solv}^{(7)}$, calculated with other basis sets, are summarized in Tables 5−7. The case of the dominant isotope ^7Li is calculated.

The solvation energies $\Delta E_{solv}^{(7)}$ and the Gibbs' functions $\Delta G_{solv}^{(7)}$ become progressively smaller, up to $n = 4$, and take almost the same value at $n = 5$ and $n = 6$. This result is attributed to the first shell being saturated at $n = 4$, and the external shell beginning to form with hydrogen bonds at $n = 5$. The solvation energies $\Delta E_{solv}^{(7)}(n = 5)$ and $\Delta E_{solv}^{(7)}(n = 6)$ are much more than twice the dimerization energy in all three solvent clusters. The Li^+−Solv bonding is stronger than the hydrogen bond, and the $4+q$ isomer is more stable than the $3+q$ and $2+q$ isomers with the cyclic structure. Furthermore, we believe that the binding energies for $n = 5$ and 6 are due to not only the two hydrogen bonds, but also the polarized solvent molecule in the first shell being bound to the Li ion, even in the $Li^+(H_2S)_n$ clusters with weak Li−S and hydrogen bonds.

One interesting point is that $Li^+(H_2O)_n$ and $Li^+(CH_3OH)_n$ give almost equal values in both $\Delta E_{solv}^{(7)}$ and $\Delta G_{solv}^{(7)}$. There is almost no influence on the binding between lithium and oxygen when one H atom in the water molecule is replaced by the methyl group. The solvation energy of the Li cation with the dimethyl ether clusters $Li^+(CH_3OCH_3)_n$ for $n = 1$, 2, 3, and 4 are 166, 137, 95, and 54 kJ/mol, respectively, at the HF/6-31+G* level,[29] and these energies are also almost equal to the solvation energies of $Li^+(H_2O)_n$ and $Li^+(CH_3OH)_n$. The methyl group replacement of even both H atoms does not significantly influence the binding energies of the Li^+−O bond. In contrast, $Li^+(H_2S)_n$ shows smaller values in both $\Delta E_{solv}^{(7)}$ and $\Delta G_{solv}^{(7)}$, because of the weaker Li^+−S bonding.

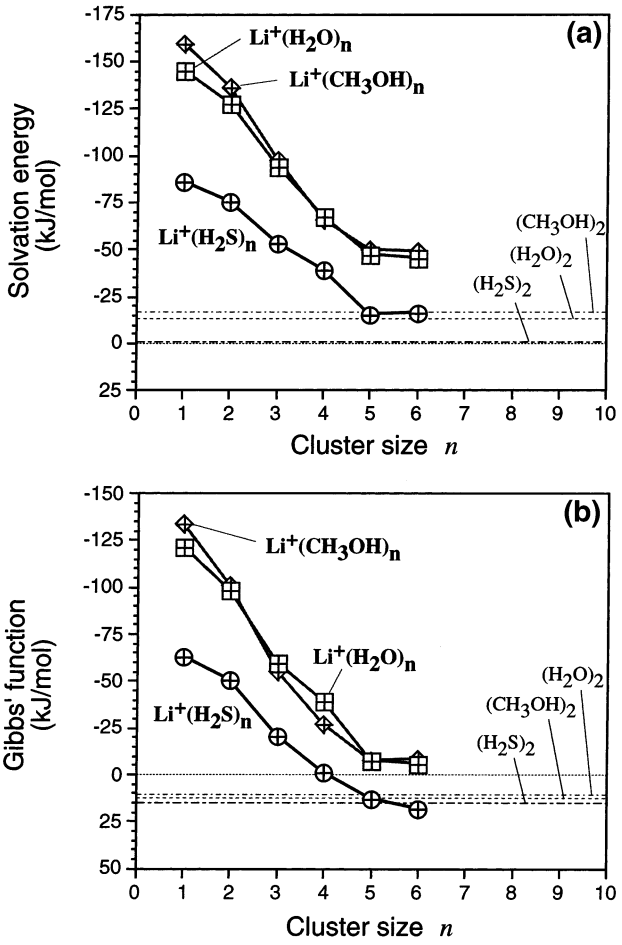

Figure 8. Size dependence of (a) the solvent energy with the zero-point vibration correction $\Delta E_{solv}^{(7)}(n)$ and (b) the Gibbs' function ($\Delta G_{solv}^{(7)}(n)$) at 298.15 K for the dominant isotope ^7Li. The most-stable isomers are used in each size n for the evaluation. Horizontal broken lines are the dimerization energies of $(H_2O)_2$, $(CH_3OH)_2$, and $(H_2S)_2$. Basis set used is the HF/6-31+G* level.

It seems that $Li^+(H_2O)_n$ can continue to make the second hydration shell with hydrogen bonds, to at least $n = 12$.[18,26,27] In contrast, the second solvation shell of the $Li^+(CH_3OH)_n$ is assumed to be saturated for $n \geq 7$, because there are no more free OH groups of methanol molecules in the first shell for $n = 6$. (See Figure 6.) Hence, it is assumed that the solvation energies $\Delta E_{solv}^{(7)}(n)$ of $Li^+(CH_3OH)_n$ for large n are smaller than those of $Li^+(H_2O)_n$, and that the enthalpy change $\Delta H_{solv}(Li^+(CH_3OH)_n) - \Delta H_{solv}(Li^+(H_2O)_n)$ is negative, as was assumed in ref 30.

3.3. Reduced Partition Function Ratio. *3.3.1. Bigeleisen and Mayer's Theory.* As is shown in the Introduction, the reduced partition function ratio (RPFR, f) is given by Bigeleisen and Mayer's theory, as follows:

$$f = \sum_i \frac{u_{i,(7)} e^{-u_{i,(7)}/2}(1 - e^{-u_{i,(6)}})}{u_{i,(6)} e^{-u_{i,(6)}/2}(1 - e^{-u_{i,(7)}})} \quad (4)$$

TABLE 5: Solvent Energy without and with the Zero-Point Vibration Energy Correction ($\Delta E_{solv}(n)$ and $\Delta E^{(7)}_{solv}$) and the Gibbs' Function ($\Delta G^{(7)}_{solv}$) for the Reaction $Li^+(H_2O)_{n-1} + H_2O \rightarrow Li^+(H_2O)_n$[a]

	HF/6-31+G*			HF/6-31+G**			HF/6-311+G*		
	ΔE_{solv}	$\Delta E^{(7)}_{solv}$	$\Delta G^{(7)}_{solv}$	ΔE_{solv}	$\Delta E^{(7)}_{solv}$	$\Delta G^{(7)}_{solv}$	ΔE_{solv}	$\Delta E^{(7)}_{solv}$	$\Delta G^{(7)}_{solv}$
$(H_2O)_2$	−22.51	−12.87	+10.47	−21.07	−11.94	+10.90	−21.87	−15.59	+8.15
$Li^+(H_2O)$	−153.63	−144.81	−120.59	−151.71	−142.81	−118.61	−164.18	−154.30	−130.00
$Li^+(H_2O)_2$	−135.45	−126.87	−97.71	−133.57	−124.94	−95.56	−144.06	−134.41	−104.78
$Li^+(H_2O)_3$	−102.91	−93.75	−58.89	−101.10	−91.85	−56.93	−111.07	−100.56	−64.85
$Li^+(H_2O)_4$	−73.74	−67.38	−39.22	−72.05	−65.38	−35.68	−79.50	−72.63	−45.71
$Li^+(H_2O)_5$	−59.96	−46.27	−6.89	−57.08	−44.26	−6.85	−64.29	−50.36	−10.29
$Li^+(H_2O)_6$	−55.93	−44.82	−5.04	−53.84	−42.95	−3.15	−60.91	−48.68	−7.36

[a] The case of the dominant isotope ^7Li is calculated for $\Delta E^{(7)}_{solv}$ and $\Delta G^{(7)}_{solv}$. The Gibbs' function is evaluated at room temperature (298.15 K), under the assumption of the ideal gas. The relative energies and the Gibbs' function for the dimerization of water are also shown.

TABLE 6: Solvent Energies (ΔE_{solv} and $\Delta E^{(7)}_{solv}$) and Gibbs' Function ($\Delta G^{(7)}_{solv}$) of the Reaction $Li^+(H_2S)_{n-1} + H_2S \rightarrow Li^+(H_2S)_n$ for the Dominant Isotope ^7Li[a]

	HF/6-31+G*			HF/6-31+G**			HF/6-311+G*		
	ΔE_{solv}	$\Delta E^{(7)}_{solv}$	$\Delta G^{(7)}_{solv}$	ΔE_{solv}	$\Delta E^{(7)}_{solv}$	$\Delta G^{(7)}_{solv}$	ΔE_{solv}	$\Delta E^{(7)}_{solv}$	$\Delta G^{(7)}_{solv}$
$(H_2S)_2$	−3.68	−0.49	+14.01	−3.83	−0.49	+15.13	−4.47	−0.77	+15.71
$Li^+(H_2S)$	−92.51	−85.07	−62.72	−92.11	−84.86	−62.52	−98.33	−90.82	−68.30
$Li^+(H_2S)_2$	−81.54	−74.73	−50.18	−81.15	−74.27	−45.67	−85.86	−78.51	−49.18
$Li^+(H_2S)_3$	−59.80	−53.05	−20.16	−59.30	−52.92	−24.60	−61.32	−54.92	−25.69
$Li^+(H_2S)_4$	−44.51	−39.12	−0.99	−44.11	−38.75	−0.01	−45.43	−39.90	−0.13
$Li^+(H_2S)_5$	−19.17	−14.86	+13.13	−19.11	−14.73	+13.94	−19.14	−15.62	+7.99
$Li^+(H_2S)_6$	−19.79	−15.75	+18.32	−19.78	−15.77	+17.74	−20.27	−16.08	+16.93

[a] The Gibbs' function is evaluated at room temperature (298.15 K), under the assumption of the ideal gas. The relative energies and the Gibbs' function for the dimerization of H_2S are also shown.

TABLE 7: Solvent Energies (ΔE_{solv} and $\Delta E^{(7)}_{solv}$) and Gibbs' Function $\Delta G^{(7)}_{solv}$ of the Reaction $Li^+(CH_3OH)_{n-1} + CH_3OH \rightarrow Li^+(CH_3OH)_n$ for the Dominant Isotope ^7Li[a]

	Basis Set (*)			HF/6-31+G*		
	ΔE_{solv}	$\Delta E^{(7)}_{solv}$	$\Delta G^{(7)}_{solv}$	ΔE_{solv}	$\Delta E^{(7)}_{solv}$	$\Delta G^{(7)}_{solv}$
$(MeOH)_2$	−22.43	−16.63	+13.08	−22.25	−16.62	+12.50
$Li^+(MeOH)$	−172.06	−165.40	−139.83	−165.50	−150.55	−132.95
$Li^+(MeOH)_2$	−147.14	−141.06	−106.46	−141.75	−135.46	−100.78
$Li^+(MeOH)_3$	−106.23	−99.79	−56.99	−102.98	−96.53	−54.40
$Li^+(MeOH)_4$	−70.18	−66.38	−30.05	−69.26	−64.91	−28.19
$Li^+(MeOH)_5$	−60.63	−51.45	−7.06	−58.54	−49.63	−7.34
$Li^+(MeOH)_6$	−56.35	−49.32	−9.51	−55.30	−48.14	−7.95

[a] The Gibbs' function is evaluated at room temperature (298.15 K), under the assumption of the ideal gas. The basis set (*) is the 6-31G set on the CH_3 groups of the methanol and the 6-31+G* sets on the other atoms. The relative energies and the Gibbs' function for the dimerization of methanol are also shown.

where

$$u_i = \left(\frac{h}{k_B T}\right)\omega_i$$

and the indices (6) and (7) correspond to the isotopes ^6Li and ^7Li, respectively. The computed normal frequencies ω_i for all i with the ab initio MO calculation are scaled and inserted into eq 4 to evaluate the RPFR (f) of the clusters.

We calculated the size dependence of the RFPR for the most-stable isomers (n+0 structure, up to $n = 4$, and 4+q structure for $n \geq 5$) of three types of $Li^+(Solv)_n$ (for Solv = H_2O, CH_3OH, and H_2S), as shown in Figure 9. The calculation level is HF/6-31+G*, and the temperature is 300 K. The RPFRs computed by eq 4 are shown by the thick solid lines with large crosses. The numerical data are summarized in Table 8 evaluated at all calculation levels.

In $Li^+(H_2O)_n$ and $Li^+(H_2S)_n$, the increment of RPFR is steep, up to $n = 3$, and becomes gentle from $n = 3$ to $n = 4$. The RPFR plateaus for $n \geq 4$. However, in $Li^+(CH_3OH)_n$, the RPFR increases steeply, up to $n = 3$, and plateaus for $n \geq 3$. The greatest contribution to the isotope exchange reaction of lithium is by the bonds between lithium and solvent molecules, and the solvent number of the first shell is significant. The first shell of the most-stable isomer is saturated by four solvent molecules; therefore, we can assume that the RPFR remains constant for $n \geq 4$. As discussed in the previous section, we believe that the most-stable isomer has a 4+q structure in the still-larger cluster size n. Consequently, the flat RPFR can be regarded as the RPFR for the bulk solution, and we can therefore estimate the RPFR to be $f = 1.07$ for $Li^+(H_2O)_n$ and $Li^+(CH_3OH)_n$ and $f = 1.03$ for $Li^+(H_2S)_n$.

Because of the almost-equal binding energy of Li−O, the systems of $Li^+(H_2O)_n$ and $Li^+(CH_3OH)_n$ show almost-equal RPFRs. In contrast, because the Li−S bond is weaker than the Li−O bond, the RPFR of $Li^+(H_2S)_n$ is smaller than that of the other two.

3.3.2. Simplified Bigeleisen and Mayer's Theory. A simplified formula for Bigeleisen and Mayer's theory is also known to exist. This formula can be applied only to an isotopic atom that is surrounded symmetrically by identical atoms:[9]

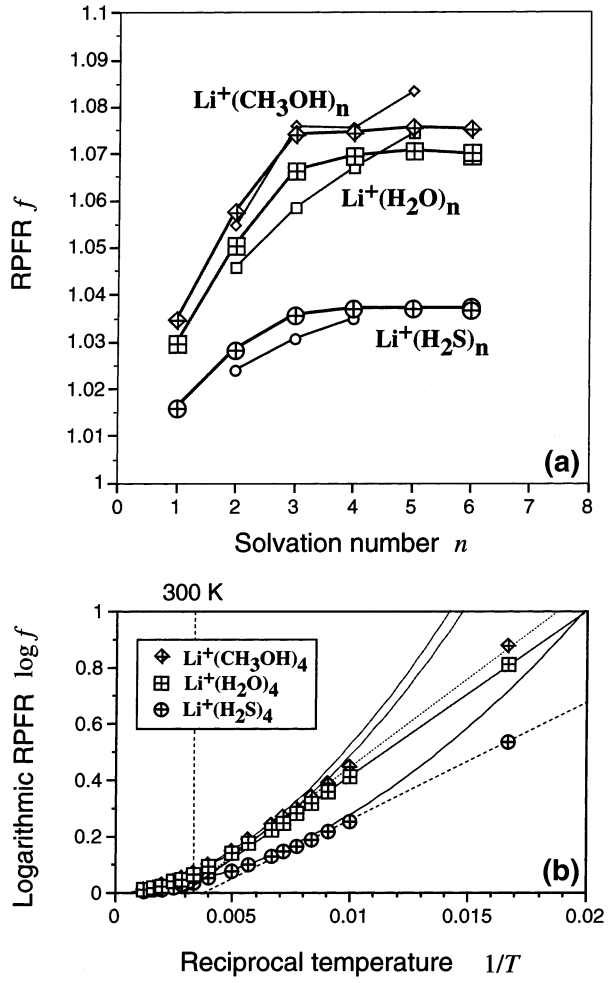

Figure 9. (a) Size dependence of the reduced partition function ratio (RPFR) of the most-stable isomers of $Li^+(H_2O)_n$, $Li^+(H_2S)_n$, and $Li^+(CH_3OH)_n$, evaluated by Bigeleisen and Mayer's formula (eq 4) together with the simplified formula (eq 5).[9] Plots of the RPFRs calculated with eq 4 are shown as thick solid lines and data points with crosses, whereas plots of the RPFRs calculated with eq 5 are shown as thin solid lines and data points without crosses. (b) Logarithmic RPFR (log *f*) versus the reciprocal absolute temperature (1/*T*) for the most-stable isomers (4+0 structure) of $Li^+(H_2O)_4$, $Li^+(H_2S)_4$, and $Li^+(CH_3OH)_4$. Frequencies were computed at the HF/6-31+G* level and multiplied by the scaling factor.

$$f_a = 1 + \left[\frac{(\Delta M)m}{24M(M+\Delta M)}\right]u_n^2 n \qquad (5)$$

where

$$u_n = \left(\frac{h}{k_B T}\right)\omega_{n,(s)}$$

and $\omega_{n,(s)}$ is the frequency of the total symmetric stretching mode of the cluster size *n*. It is known that the logarithmic RPFR (log *f*) is proportional to 1/*T* in the low-temperature region, whereas log *f* is proportional to $1/T^2$ in the higher-temperature region. This simplified formula is valid in the higher-temperature region only.

Because all the isomers give the same result, we show the temperature dependence for only the 4+0 structure of $Li^+(Solv)_4$. The logarithmic RPFR (log *f*) versus reciprocal temperature (1/*T*) is shown in Figure 9b, and, as the figure shows, room temperature is located in the higher-temperature region.

We incorporated the RPFRs evaluated by the simplified theory to Figure 9a. They are shown as thin solid lines and plots without crosses. Numerical data for all calculation levels are summarized in Table 9, together with the frequency of the total symmetric stretching motion ($\omega_{n,(s)}$). Equation 5 can be applied only to an isotopic atom that is surrounded by identical particles; values of the *n*+0 structure for $n \geq 2$ are shown. In the case of $Li^+(H_2S)_n$, the values obtained from the simplified theory are very similar to the values evaluated with the formula, utilizing all frequencies in eq 4. For $Li^+(H_2O)_n$, the simple theory shows good estimation for $n = 2$ and 4, but underestimates $n = 3$. In contrast, in $Li^+(CH_3OH)_n$, the RPFR of the simplified formula is in excellent agreement with the RPFR derived from all frequencies.

Table 9 shows that $\omega_{n,(s)}$ exhibits a gradual red shift, relative to increasing cluster size *n*. The red shift from $\omega_{2,(s)}$ to $\omega_{3,(s)}$ in $Li^+(CH_3OH)_n$ is not so large (274 cm^{-1} to 264 cm^{-1} with HF/6-31+G* versus 250 cm^{-1} to 231 cm^{-1} for $Li^+(H_2O)_n$.) Hence, $\omega_{3,(s)}$ of $Li^+(CH_3OH)_3$ retains a large value, and we believe that the simplified theory gives excellent agreement for $Li^+(CH_3OH)_3$.

TABLE 8: Reduced Partition Function Ratios (RPFRs) for $Li^+(H_2O)_n$, $Li^+(H_2S)_n$, and $Li^+(CH_3OH)_n$, Calculated by Bigeleisen and Mayer's Formula (eq 4), Using All Computed Frequencies with the Hartree−Fock (HF) Level

		RPFR Value			
	p+*q*	basis set (*)[a]	6-31+G*	6-31+G**	6-311+G*
$Li^+(H_2O)_1$	1+0		1.030	1.029	1.031
$Li^+(H_2O)_2$	2+0		1.050	1.050	1.052
$Li^+(H_2O)_3$					
3-a	3+0		1.066	1.065	1.071
3-b	2+1		1.056	1.055	1.058
$Li^+(H_2O)_4$					
4-a	4+0		1.069	1.068	1.072
4-b	3+1		1.068	1.067	1.074
4-c	2+2		1.057	1.056	1.059
$Li^+(H_2O)_5$					
5-a	4+1		1.070	1.069	1.074
5-b	3+2		1.071	1.070	1.076
5-c	3+2		1.069	1.068	1.075
5-d	5+0		1.056	1.053	1.061
5-e	2+3		1.058	1.057	1.060
$Li^+(H_2O)_6$					
6-a	4+2		1.070	1.068	1.074
6-b	4+2		1.070	1.068	1.074
6-c	3+3		1.073	1.072	1.078
6-d	3+3		1.072	1.071	1.076
6-e	3+3		1.070	1.069	1.075
$Li^+(H_2S)_1$	1+0		1.016	1.016	1.018
$Li^+(H_2S)_2$	2+0		1.028	1.028	1.033
$Li^+(H_2S)_3$	3+0		1.036	1.035	1.039
$Li^+(H_2S)_4$					
4-a	4+0		1.037	1.037	1.039
4-b	3+1		1.036	1.036	1.040
$Li^+(H_2S)_5$	4+1		1.037	1.036	1.039
$Li^+(H_2S)_6$					
6-a	4+2		1.037	1.037	1.040
6-b	4+2		1.037	1.037	1.039
$Li^+(MeOH)_1$	1+0	1.035	1.034		
$Li^+(MeOH)_2$	2+0	1.059	1.057		
$Li^+(MeOH)_3$					
3-a	3+0	1.077	1.074		
3-b	2+1	1.065	1.063		
$Li^+(MeOH)_4$					
4-a	4+0	1.076	1.074		
4-b	3+1	1.078	1.076		
$Li^+(MeOH)_5$					
5-a	4+1	1.077	1.075		
5-b	3+2	1.079	1.076		
5-c	5+0	1.057	1.055		
$Li^+(MeOH)_6$	4+2	1.077	1.075		

[a] The basis sets (*) involve putting HF/6-31+G on the methyl group of the methanol molecule and HF/6-31+G* on the remaining atoms.

TABLE 9: Reduced Partition Function Ratio (RPFR) Estimated with the Simplified Bigeleisen and Mayer's Formula (eq 5)[a]

	Basis Sets (*)[a]		HF/6-31+G*		HF/6-31+G**		HF/6-311+G*	
	$\omega_{n,(s)}$	RPFR, f_a	$\omega_{n,(s)}$	RPFR, f_a	$\omega_{n,(s)}$	RPFR, f_a	$\omega_{n,(s)}$	RPFR, f_a
$Li^+(H_2O)_2$			250	1.046	249	1.045	256	1.048
$Li^+(H_2O)_3$			231	1.058	230	1.058	238	1.062
$Li^+(H_2O)_4$			214	1.067	212	1.065	227	1.075
$Li^+(H_2O)_5$			202	1.074	198	1.072	205	1.076
$Li^+(H_2S)_2$			128	1.024	128	1.024	138	1.028
$Li^+(H_2S)_3$			119	1.031	119	1.031	126	1.035
$Li^+(H_2S)_4$			109	1.035	109	1.035	116	1.039
$Li^+(MeOH)_2$	277	1.056	274	1.055				
$Li^+(MeOH)_3$	264	1.076	264	1.076				
$Li^+(MeOH)_4$	230	1.077	227	1.075				
$Li^+(MeOH)_5$	215	1.084	214	1.083				

[a] The frequency of the total symmetric stretching mode ω_1 (cm^{-1}) is also shown in the table. The basis sets (*) for $Li^+(CH_3OH)_n$ involve putting HF/6-31+G on the methyl group of the methanol molecule and HF/6-31+G* on the remaining atoms.

The value for the 5+0 isomer is calculated in the case of $n = 5$. As will be mentioned in the next subsection (Section 3.3.3), the RPFR evaluated with all frequencies (in eq 4) for the 5+0 structure is smaller than that of the 4+1 structure in both $Li^+(H_2O)_5$ and $Li^+(CH_3OH)_5$. The equation, which is based on the simple theory, gives a gross overestimation for $n = 5$. It seems that this overestimation is attributable to the weaker Li−Solv bond and to the solvent molecules not being completely equivalent in the 5+0 isomer.

The frequency of the symmetric stretching mode remains constant as $\omega_{n,(s)} = \sqrt{k/m}$, where m is the mass of the solvent molecule and k is the force constant of the Li^+−Solv bonding. If the force constant k is not variable, the frequency is independent of the cluster size n. In the actual cluster, however, the binding energy of Li^+−Solv becomes progressively smaller, and the frequency $\omega_{n,(s)}$ shows a red shift, relative to increasing cluster size n.

3.3.3. Isomer Dependence. The RPFR value of the lithium isotopic exchange reaction is predominantly determined by the coordination number of the first solvent shell. To inspect this determination better, we will discuss the isomer dependence of the RPFR value. Figure 10 shows the plots of the RPFR of $Li^+(H_2O)_n$, $Li^+(CH_3OH)_n$, and $Li^+(H_2S)_n$ calculated for each isomer. The numerical data are summarized in Table 8.

In some cases, we found several isomers for the same $p+q$ structure. For example, three types of isomers were observed for the 3+3 structure of $Li^+(H_2O)_6$. Their RPFRs are almost equal, and it is impossible to distinguish these plots on a graph. Hence, the RPFR is independent of the structure of the second and the external solvent shell.

We can conclude that the RPFRs are dependent only on the coordination number of the first solvent shell. For $Li^+(H_2O)_n$ and $Li^+(CH_3OH)_n$, the $3+q$ and $4+q$ isomers show almost-equal RPFRs, and they give the largest possible RPFR, with respect to isomer dependence. Of the other types of isomers, the $2+q$ and $5+q$ structures give smaller RPFRs. The variation among the isomers is very small in $Li^+(H_2S)_n$, and the number of RPFR plots is also very few; however, the RPFRs of $3+q$ and $4+q$ isomers are almost equal.

As discussed previously, the most-stable isomers have a $4+q$ structure, up to $n = 6$, whereas the next-stable isomers have a $3+q$ structure. In particular, the stability of $Li^+(H_2O)_6$ at room temperature is mostly determined by the number of solvent molecules in the first shell. Thus, we can assume that the $4+q$ and $3+q$ structures are the most stable for the much larger clusters, and we can guess that many cases exist for which the coordination number is 3 or 4 in the bulk solution also. Finally, the RPFRs for the clusters up to $n = 6$ can be extrapolated to the bulk solution, and we can conclude that the RPFR is 1.07 for water and methanol and 1.03 for H_2S.

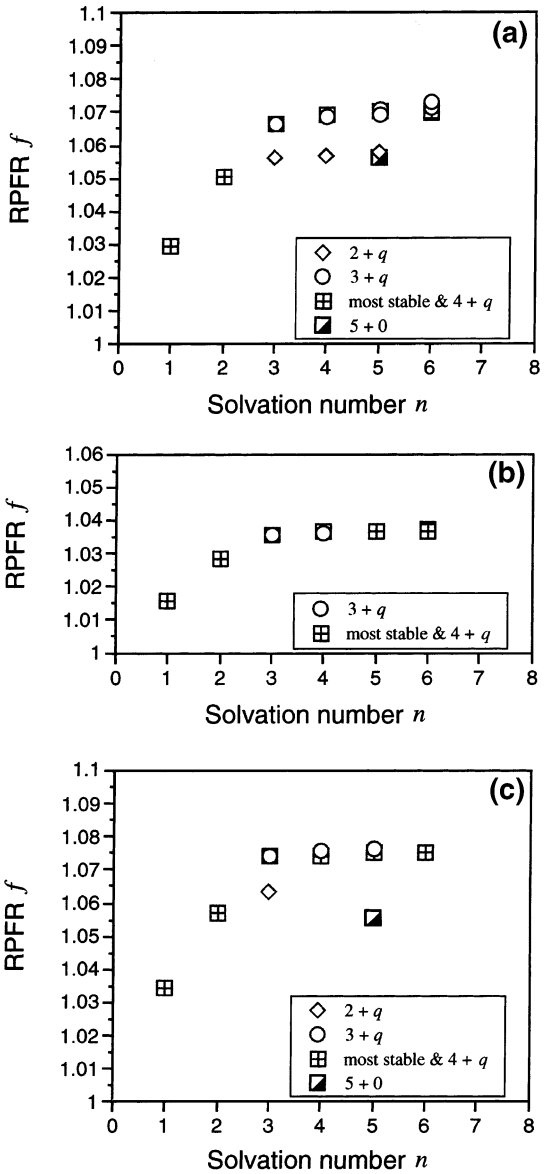

Figure 10. Isomer dependence of the RPFR, calculated by Bigeleisen and Mayer's formula (eq 4): (a) $Li^+(H_2O)_n$, (b) $Li^+(H_2S)_n$, and (c) $Li^+(CH_3OH)_n$. Frequencies were calculated at the HF/6-31+G* level and multiplied by the scaling factor.

3.4. Analysis of Vibration Mode. In this subsection, we inspect the vibration mode that contributes significantly to the

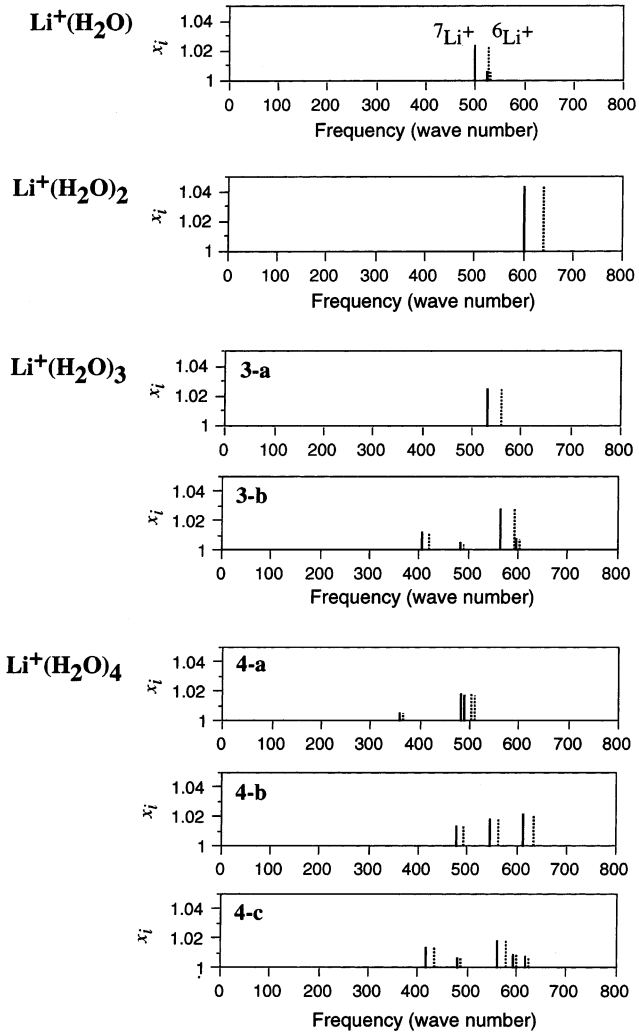

Figure 11. Frequency versus contribution to the RPFR of x_i for $Li^+(H_2O)_n$, up to $n = 4$. Basis set for the computation used is the HF/6-31+G* level. Modes with a significant contribution ($x_i \geq 1.005$) are shown. The frequencies 533 cm^{-1} (of $^7Li(H_2O)_3$ isomer **3-a**) and 484 cm^{-1} (of $^7Li(H_2O)_4$ isomer **4-a**) are doubly degenerated.

reduced partition function ratio (RPFR). Figures 11−13 show the normal frequency taken as the abscissa and the contribution to RPFR (x_i) taken as the ordinate, up to $n = 4$. The contribution x_i is shown by the following formula:

$$x_i = \frac{u_{i,(7)} e^{-u_{i,(7)}/2}(1 - e^{-u_{i,(6)}})}{u_{i,(6)} e^{-u_{i,(6)}/2}(1 - e^{-u_{i,(7)}})} \qquad (6)$$

where

$$u_i = \left(\frac{h}{k_B T}\right)\omega_i$$

The frequencies whose x_i value is significantly large are shown in the figure. We have shown the frequency of the dominant isotope ^7Li as solid lines and that of the minor isotope ^6Li as broken lines. The frequency list for all optimized geometries are available on request.[37]

3.4.1. Isomers of n+0 Structure up to n = 4. The vibration mode whose contribution x_i is significant for $n = 1$ is the stretching motion between the Li ion and the solvent molecule (Solv). The frequency is also linked to the binding energy of the Li^+−Solv bond. In the major isotope ^7Li, the frequencies

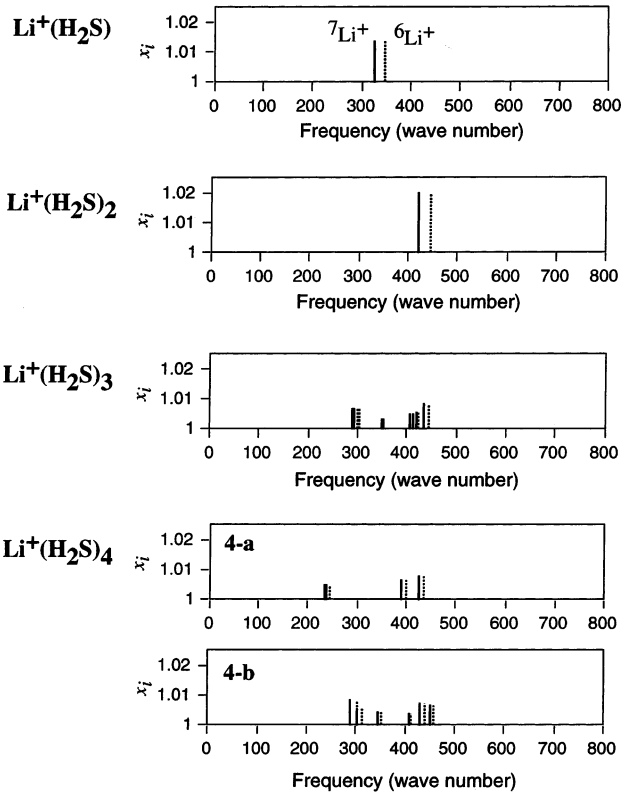

Figure 12. Frequency versus contribution to the RPFR of x_i for $Li^+(H_2S)_n$, up to $n = 4$. Basis set used is the HF/6-31+G* level. Modes with a significant contribution ($x_i \geq 1.0025$) are shown. The frequencies 235 and 391 cm^{-1} of $^7Li(H_2S)_4$ isomer **4-a** are doubly degenerated.

for $Li^+(H_2O)$ and $Li^+(CH_3OH)$ are 500 and 526 cm^{-1}, whereas the frequency for $Li^+(H_2S)$ is 326 cm^{-1}. (In the following discussion, the numerical frequency values are shown for ^7Li, because the difference of the frequencies between ^7Li and ^6Li are so similar, to be proportional to x_i.)

Because the vibration mode that involves the Li^+−Solv bond is significant, the antisymmetric stretching motion contributes dominantly to the RPFR. The frequencies of the antisymmetric stretching motion of $Li^+(H_2O)_2$, $Li^+(CH_3OH)_2$, and $Li^+(H_2S)_2$, are 599, 629, and 420 cm^{-1}, respectively, and a blue shift occurs from $n = 1$ to $n = 2$ in all three clusters. It can be simply understood as a classic coupled oscillator system. Supposing the masses of the Li atom and the solvent molecule are M and m respectively, and the force constant is k, then the frequencies of $n = 1$ and 2 become $\omega_1 = \sqrt{k(M+m)/(Mm)}$ and $\omega_{2,(a)} = \sqrt{k(M+2m)/(Mm)}$, and we can obtain the relation of $\omega_1 < \omega_{2,(a)}$.

In the n+0 structure for $2 \leq n \leq 4$, the frequency of the antisymmetric stretching mode shows a gradual red shift. It is also attributed to the binding energy of the Li^+−Solv bond becoming progressively smaller with increasing cluster size n. The red shift of $Li^+(H_2S)_n$ (414 cm^{-1} for $n = 2$, 391 and 426 cm^{-1} for $n = 4$) is smaller than that of $Li^+(H_2O)_n$ (599 cm^{-1} for $n = 2$, 484 and 491 cm^{-1} for $n = 4$) and $Li^+(CH_3OH)_n$ (629 cm^{-1} for $n = 2$, 413, 448, and 454 cm^{-1} for $n = 4$).

3.4.2. Frequency Distribution and Frequency Shift. The distribution of the frequencies with large x_i values is dependent predominantly on the structure of the first solvation shell, and the frequency shift is dependent on the strength of the Li^+−Solv bonding. In some cases, the second solvation shell constructed with the hydrogen bond influences the first solvation

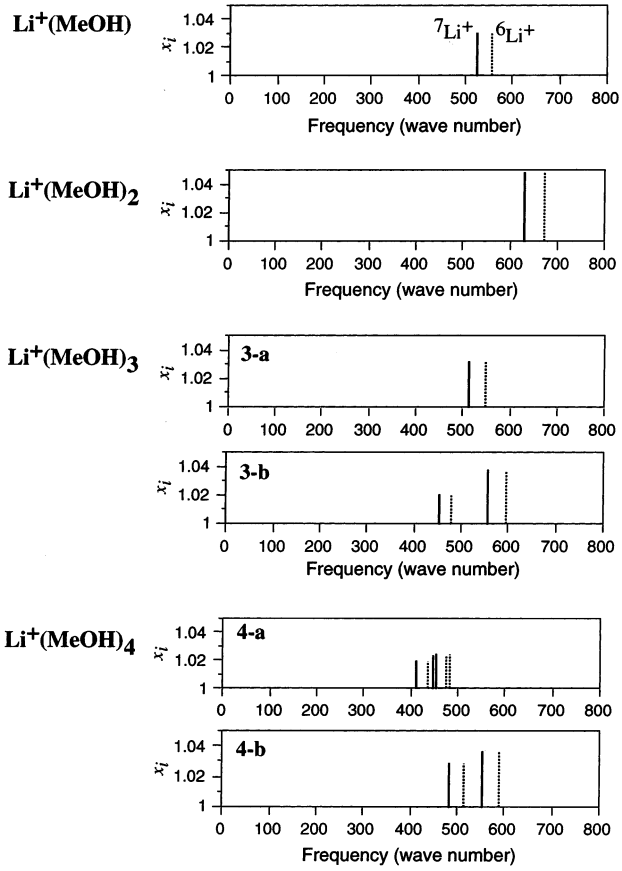

Figure 13. Frequency versus contribution to the RPFR of x_i for $Li^+(CH_3OH)_n$, up to $n = 4$. Basis set used is the HF/6-31+G* level. Modes with a significant contribution ($x_i \geq 1.005$) are shown. The frequency 512 cm^{-1} of $^7Li(CH_3OH)_3$ isomer **3-a** is doubly degenerated.

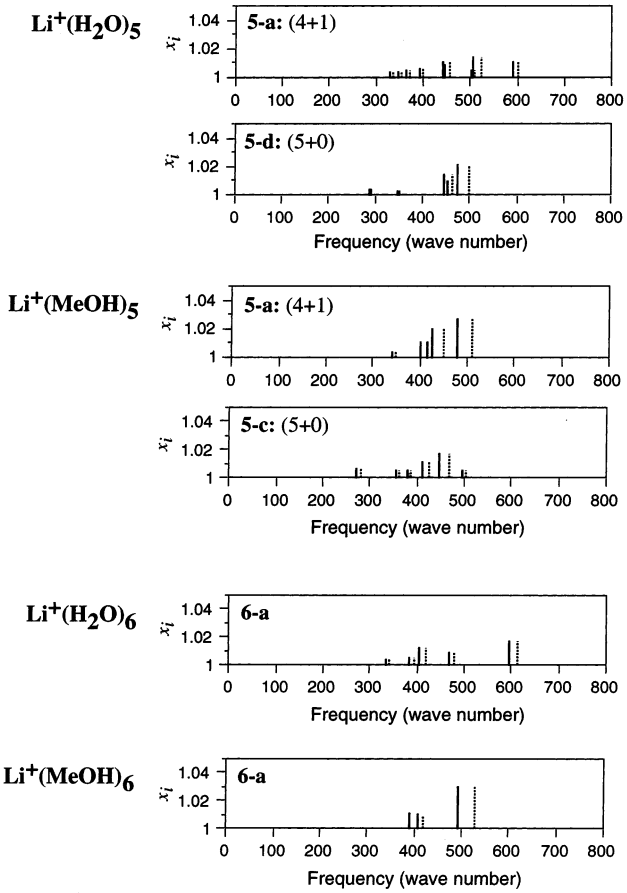

Figure 14. Frequency versus contribution to the RFPR of x_i for several isomers of $Li^+(H_2O)_n$ and $Li^+(CH_3OH)_n$ ($n = 5$ and 6). Modes with $x_i \geq 1.0025$ are shown. The frequencies 334, 386, and 468 cm^{-1} (of $^7Li^+(H_2O)_6$) and 392 and 409 cm^{-1} (of $^7Li(CH_3OH)_6$) are doubly degenerated.

shell, and the distribution and the shift of the frequency is indirectly dependent on the second solvation shell.

In the $Li^+(H_2O)_3$ isomer **3-b**, the mode with the frequency 565 cm^{-1} is identified as the antisymmetric stretching motion of the O−Li^+−O bond, and the bending motion with the frequency 405 cm^{-1} also gives a somewhat large x_i value. Because of the similar cyclic structure, the frequency distribution of the $Li^+(H_2O)_4$ isomer **4-c** has a pattern similar to that of isomer **3-b**. The three water molecules in isomer **3-a** are equivalent and the two antisymmetric stretching modes degenerate (533 cm^{-1}), whereas in isomer **4-b**, the two antisymmetric stretching modes do not degenerate (611 and 475 cm^{-1}), because of the influence of the second hydration shell. The mode with the frequency 544 cm^{-1} in isomer **4-b** is identified as the bending motion, the same as in isomer **3-b**. The frequencies of isomer **4-b** are blue-shifted from the frequencies of isomer **3-b**, because the hydrogen bond in isomer **4-b** (2.033 Å) is stronger than that in isomer **3-b** (2.047 Å).

We have described only the case of the $Li^+(H_2O)_n$ cluster in this paragraph. The $Li^+(H_2S)_n$ and the $Li^+(CH_3OH)_n$ clusters can be also explained with the same analysis.

3.4.3. Larger Clusters. Finally, the frequencies versus the x_i values of $Li^+(H_2O)_n$ and $Li^+(CH_3OH)_n$ for $n = 5$ and 6 are shown in Figure 14. The isomers of the most-stable 4+1 and 5+0 structures are shown for $n = 5$, and the most-stable 4+2 structure is shown for $n = 6$. The contribution of x_i of the most-stable isomers is very similar to that of the 4+0 isomers of $Li^+(H_2O)_4$ and $Li^+(CH_3OH)_4$. On the other hand, the x_i value of the 5+0 isomers is small in both $Li^+(H_2O)_5$ and $Li^+(CH_3OH)_5$. We believe that this phenomenon can be attributed to the RPFR of the 5+0 isomer becoming smaller than that of the 4+1 isomer, as calculated with all frequencies. The frequency of the total symmetric stretching mode $\omega_{5,(s)}$ shows a red shift from the frequency of $n = 4$; however, the degree of the shift is not so significant (see Table 9). Therefore, the simplified theory gives an overestimation of the RPFR for $n = 5$.

4. Conclusion and Remarks

In the present study, we determined the structures of three types of solvent lithium ion clusters $Li^+(Solv)_n$ (in which Solv = H_2O, H_2S, and CH_3OH) with an ab initio molecular orbital (MO) method. The reduced partition function ratio (RPFR) values of the bulk solution in the lithium isotope exchange reaction were estimated on the basis of the calculated RPFRs of these three clusters.

The Li^+−Solv bond primarily determines the RPFR; therefore, it is predominantly dependent on the number of solvent molecules in the first shell. In all three clusters, the most-stable isomer has a 4+q structure for $n \geq 4$; thus, the size dependence of the RPFR plateaus at $n = 4$. Therefore, the extrapolation of the cluster value can be regarded as the RPFR of the bulk solution, and, consequently, we can estimate the RPFR to be 1.07 for water and methanol and 1.03 for H_2S.

It is known that the scaling factor does not work very well for low-frequency modes such as the symmetric stretching mode that involves the Li^+−Solv bond.[13,26,27] Fortunately, the majority of the zero-point energies are determined by the energy relation $E = {}^1/_2h\nu$. The isotope-dependent frequencies that involve the

large displacement of lithium would be sensitive to the scaling factor, especially after exponentiation in the partition function. However, the possibility remains that the use of the ratio of partition function might cause the scaling factor to cancel.

As described in Section 3.4, the antisymmetric stretching mode contributes predominantly to the RPFR. In general, the scaling factor works for the antisymmetric stretching mode better than for the symmetric stretching mode. The distribution and shift of the frequencies with the large contribution of x_i are clearly dependent on the first solvation shell and the binding energy of the Li^+-Solv bond. Given these regularities, the shape of the potential curve may not be significantly influenced in the case of the antisymmetric stretching mode. Therefore, the valid RPFRs are assumed to be obtained by the uniformed scaling factor.

The $3+q$ structure is the next-stable isomer, relative to the $4+q$ structure, as revealed in the thermodynamic discussion, and we believe that the coordination number of the lithium ion is 3 or 4 in most cases, because the $3+q$ and $4+q$ isomers give almost-equal RPFRs, and the mixing of the $3+q$ structures do not have significant influence on the RPFR of the bulk solution.

Although the 5+0 structure was observed for $n = 5$ at the HF/6-31+G* level, the local minimum does not exist at the MP2/6-31+G* level.[26] This fact suggests that the $5+q$ isomer does not have any stable local minimum or has only a very unstable minimum. We found the 6+0 structure for $n = 6$, and, because its relative energy difference is +40.9 kJ/mol with the HF/6-31+G*, and the 6+0 isomer is very unstable.[19] With regard to the stability of such overvalence clusters of the Li ion, we assume that the coordination number is 5 or 6 in small cases of the bulk solution. The calculated RPFRs for the $5+q$ and the $6+q$ isomers are small; however, the contribution of these structures is assumed to be small and, therefore, the influence on the RPFR in the bulk solution is not very significant.

The replacement of one H atom in the water molecule by a methyl group had very little influence on the Li−O bonding in the $Li^+(CH_3OH)_n$ cluster. On the other hand, the results for $Li^+(H_2S)_n$ suggest the possibility of an absorbent that contains S atoms, such as thioether, etc. We should consider the following reaction of the lithium isotopic exchange:

$$^6Li_I^+ + {}^7Li_{II}^+ \rightleftharpoons {}^7Li_I^+ + {}^6Li_{II}^+$$

where phase I is a liquid phase, such as seawater, and phase II is the absorbent that contains the S atom.

Acknowledgment. The authors wish to thank Dr. R. Takasu for giving us access to the spectroscopy of the clusters $Cs^+(CH_3OH)_n$ and $Na^+(CH_3OH)_n$. (See refs 32−34.) This study was financially supported by the Budget for Nuclear Research of the Ministry of Education, Culture, Sports, Science and Technology, based on screening and counseling by the Atomic Energy Commission.

References and Notes

(1) Symonds, E. A. *Sep. Sci. Technol.* **1985**, *20*, 633.
(2) Palko, A. A.; Drury, J. S.; Begun, G. M. *J. Chem. Phys.* **1976**, *64*, 1828.
(3) Singh, G.; Hall, J. C.; Rock, P. A. *J. Chem. Phys.* **1972**, *56*, 1855. Singh, G.; Rock, P. A. *J. Chem. Phys.* **1972**, *57*, 5556. Hall, J. C.; Silvester, L. F.; Singh, G.; Rock, P. A. *J. Chem. Phys.* **1973**, *59*, 6358.
(4) Ooi, K.; Feng, Q.; Kanoh, H.; Hirotsu, T.; Oi, T. *Sep. Sci. Technol.* **1995**, *30*, 3761.
(5) Ogino, H.; Oi, T. *Sep. Sci. Technol.* **1996**, *31*, 1215.
(6) Nishizawa, K.; Watanabe, H.; Ishino, S.; Shinagawa, M. *J. Nucl. Sci. Technol.* **1984**, *21*, 133. Nishizawa, K.; Watanabe, H. *J. Nucl. Sci. Technol.* **1986**, *23*, 843. Nishizawa, K.; Ikeda, I.; Okahara, M. *Sep. Sci. Technol.* **1988**, *23*, 333.
(7) Thomas, M. W.; Mariñas, B. J.; Fritz, S. J. *J. Membr. Sci.* **1994**, *88*, 231.
(8) Ooi, K.; Kanoh, H.; Sugihara, H.; Hiratani, K.; *Chem. Lett.* **1997**, 615.
(9) Bigeleisen, J.; Mayer, M. G. *J. Chem. Phys.* **1947**, *15*, 261.
(10) Michaelian, K. H.; Moskovits, M. *Nature* **1978**, *273*, 135.
(11) Kanno, H.; Hiraishi, J. *J. Phys. Chem.* **1983**, *87*, 3664.
(12) Kameda, Y.; Ebata, H.; Umemura, O. *Bull. Chem. Soc. Jpn.* **1994**, *67*, 929.
(13) Rudolph, W.; Brooker, M. H.; Pye, C. C. *J. Phys. Chem.* **1995**, *99*, 3793.
(14) Marcus, Y. *Chem. Rev.* **1988**, *88*, 1475.
(15) Ohtaki, H.; Radnai, Y. *Chem. Rev.* **1993**, *93*, 1157.
(16) Bischof, G.; Silbernagl, A.; Hermansson, K.; Probst, M. *Int. J. Quantum Chem.* **1997**, *65*, 803.
(17) Yanase, S.; Oi, T. *Zeit. Naturforsch. A* **2001**, *56*, 297
(18) Yanase, S.; Oi, T. *J. Nucl. Sci. Technol.* **2002**, *39*, 1060.
(19) Yamaji, K.; Makita, Y.; Watanabe, H.; Sonoda, A.; Kanoh, H.; Hirotsu, T.; Ooi, K. *J. Phys. Chem. A* **2001**, *105*, 602.
(20) Hashimoto, K.; Kamimoto, T.; Daigoku, K. *J. Phys. Chem. A* **2000**, *104*, 3299. Hashimoto, K.; Kamimoto, T.; Fuke, K. *Chem. Phys. Lett.* **1997**, *266*, 7. Hashimoto, K.; He, S.; Morokuma, K. *Chem. Phys. Lett.* **1993**, *206*, 297. Hashimoto, K.; Morokuma, K. *Chem. Phys. Lett.* **1994**, *223*, 423. Hashimoto, K.; Morokuma, K. *J. Am. Chem. Soc.* **1994**, *116*, 11436.
(21) Bauschlicher, C. W., Jr.; Langhoff, S. R.; Partridge, H.; Rice, J. E.; Komornicki, A. **1991**, *95*, 5142.
(22) Hashimoto, K.; Kamimoto, T. *J. Am. Chem. Soc.* **1998**, *120*, 3560.
(23) Feller, D.; Glendening, E. D.; Kendall R. A.; Peterson, K. A. *J. Chem. Phys.* **1994**, *100*, 4981.
(24) Glendening, E. D.; Feller, D. *J. Phys. Chem.* **1995**, *99*, 3060.
(25) Feller, D.; Glendening, E. D.; Woon, D. E.; Feyereisen, M. W. *J. Chem. Phys.* **1995**, *103*, 3526.
(26) Pye, C. C. *Int. J. Quantum Chem.* **2000**, *76*, 62.
(27) Pye, C. C.; Poirier, R. A.; Rudolph, W. *J. Phys. Chem.* **1996**, *100*, 601.
(28) Bochkarev, A. V. *Russ. J. Phys. Chem.* **2001**, *75*, 1566.
(29) More, M. B.; Glendening, E. D.; Ray, D.; Feller, D.; Armentrout, P. B. *J. Phys. Chem.* **1996**, *100*, 1605.
(30) Nielsen, S. B.; Masella, M.; Kebarle, P. *J. Phys. Chem. A* **1999**, *103*, 9891.
(31) Weinheimer, C. J.; Lisy, J. M. **1996**, *105*, 2938.
(32) Weinheimer, C. J.; Lisy, J. M. *Int. J. Mass Spectrom.* **1996**, *159*, 197.
(33) Cabarcos, O. M.; Lisy, J. M. *Chem. Phys. Lett.* **1996**, *257*, 265. Selegue, T. J.; Cabarcos, O. M.; Lisy, J. M. *J. Chem. Phys.* **1994**, *100*, 4790. Draves, J. A.; Lisy, J. M. *J. Am. Chem. Soc.* **1990**, *112*, 9006. Selegue, T. J.; Lisy, J. M. *J. Am. Chem. Soc.* **1994**, *116*, 4874.
(34) Weinheimer, C. J.; Lisy, J. M. *J. Phys. Chem.* **1996**, *100*, 15305.
(35) Online spectral database Integrated Spectral Data Base System for Organic Compounds, http://www.aist.go.jp/RIODB/SDBS/menu-e.html. Yamamoto, O.; Someno, K.; Wasada, N.; Hiraishi, J.; Hayamizu, K.; Tanabe, K.; Tamura, T.; Yanagisawa, M. An Integrated Spectral Data Base System Including IR, MS, ^{1}H NMR, ^{13}C NMR, ESR and Raman Spectra. *Anal. Sci.* **1998**, *4*, 233.
(36) Frisch, M. J.; Trucks, G. W.; Schlegel, H. B.; Scuseria, G. E.; Robb, M. A.; Cheeseman, J. R.; Zakrzewski, V. G.; Montgomery, J. A., Jr.; Stratmann, R. E.; Burant, J. C.; Dapprich, S.; Millam, J. M.; Daniels, A. D.; Kudin, K. N.; Strain, M. C.; Farkas, O.; Tomasi, J.; Barone, V.; Cossi, M.; Cammi, R.; Mennucci, B.; Pomelli, C.; Adamo, C.; Clifford, S.; Ochterski, J.; Petersson, G. A.; Ayala, P. Y.; Cui, Q.; Morokuma, K.; Malick, D. K.; Rabuck, A. D.; Raghavachari, K.; Foresman, J. B.; Cioslowski, J.; Ortiz, J. V.; Stefanov, B. B.; Liu, G.; Liashenko, A.; Piskorz, P.; Komaromi, I.; Gomperts, R.; Martin, R. L.; Fox, D. J.; Keith, T.; Al-Laham, M. A.; Peng, C. Y.; Nanayakkara, A.; Gonzalez, C.; Challacombe, M.; Gill, P. M. W.; Johnson, B. G.; Chen, W.; Wong, M. W.; Andres, J. L.; Head-Gordon, M.; Replogle, E. S.; Pople, J. A. *Gaussian 98*, revision A.9; Gaussian, Inc.: Pittsburgh, PA, 1998.
(37) The E-mail address for author H.W. is watanabe.h@aist.go.jp, and the E-mail address for author K.O. is k-ooi@aist.go.jp.
(38) Watanabe, H.; Iwata, S.; Hashimoto, K.; Misaizu, F.; Fuke, K. *J. Phys. Chem.* **1995**, *117*, 755.
(39) Watanabe, H.; Iwata, S. *J. Chem. Phys.* **1998**, *108*, 10078.
(40) Asada, T.; Iwata, S. *Chem. Phys. Lett.* **1996**, *260*, 1.
(41) Harms, H. C.; Khanna, S. N.; Chen, B.; Castleman, A. W., Jr. *J. Chem. Phys.* **1994**, *100*, 3540.